Interplay of disorder and $\mathcal{PT}$ symmetry in one-dimensional optical lattices

Cristian Mejía-Cortés[1,2,*] and Mario I. Molina[1]

[1]*Departamento de Física, Facultad de Ciencias, Universidad de Chile, Casilla 653, Santiago, Chile*
and Center for Optics and Photonics (CEFOP) and MSI-Nucleus on Advanced Optics, Casilla 4016, Concepcion, Chile
[2]*Grupo de Espectroscopía Óptica de Emisión y Láser, Universidad del Atlántico, Km 7 vía a Puerto Colombia, Barranquilla, Colombia*

We study a one-dimensional binary optical lattice in the presence of diagonal disorder and alternating gain and loss, and examine the light transport phenomena for localized and extended input beams. In the pure $\mathcal{PT}$-symmetric case, we derive an exact expression for the behavior of light localization in terms of typical parameters of the system. Within the $\mathcal{PT}$-symmetric region light localization becomes constant as a function of the strength of the gain and loss parameter, but outside the $\mathcal{PT}$-symmetric window, light localization increases as the gain and loss parameter increases. When disorder is added, we observe that the presence of gain and loss inhibits (favors) the transport for localized (extended) excitations.

I. INTRODUCTION

In 1958 Anderson showed, within the independent electron framework, that the presence of a finite concentration of linear uncorrelated disorder completely inhibits the quasiparticle propagation in one and two dimensions, giving rise to a saturation of its mean-square displacement and an exponential decrease of the transmissivity of plane waves with system size [1–3]. Proposed originally for electrons and one-particle excitations in solids [1,4–6], it was soon extended to many other fields such as acoustics [7,8], Bose-Einstein condensates [9], and optics [10–16].

A different and novel concept that has gained much recent attention is that of $\mathcal{PT}$ symmetry. It is based on the seminal work of Bender and co-workers [17,18], who showed that non-Hermitian Hamiltonians are capable of displaying a purely real eigenvalue spectrum, provided the system is invariant with respect to the combined operations of parity ($\mathcal{P}$) and time-reversal ($\mathcal{T}$) symmetry. For one-dimensional systems the $\mathcal{PT}$ requirement leads to the condition that the imaginary part of the potential term in the Hamiltonian be an odd function, while its real part be even. In a $\mathcal{PT}$-symmetric system, the effects of loss and gain can balance each other and, as a result, give rise to a bounded dynamics. The system thus described can experience a spontaneous symmetry breaking from a $\mathcal{PT}$-symmetric phase (all eigenvalues real) to a broken phase (at least two complex eigenvalues), as the imaginary part of the potential is increased. In the case of optics, the paraxial wave equation has the form of a Schrödinger equation and, as a consequence, the potential is proportional to the index of refraction. The $\mathcal{PT}$-symmetry requirements lead to the condition that the real part of the refractive index be an even function, while the imaginary part be an odd function in space. To date, numerous $\mathcal{PT}$-symmetric systems have been explored in several fields, from optics [19–26], electronic circuits [27], solid-state, and atomic physics [28,29], to magnetic metamaterials [30], among others. The $\mathcal{PT}$-symmetry-breaking phenomenon has been observed in several experiments [22,23,31,32]. Recently, it has been observed that

the presence of $\mathcal{PT}$ symmetry in a (discrete) one-dimensional (1D) waveguide array with binary coupling gives rise to light localization, i.e., "emulates" disorder [33].

It is known that a 1D simple periodic lattice with homogeneous couplings and endowed with gain and loss, displaying in this way $\mathcal{PT}$ symmetry, is always in the broken phase of this symmetry and does not have a stable parameter window [34]. For finite $\mathcal{PT}$-symmetrical lattices, it has been shown that $\mathcal{PT}$ symmetry is preserved inside a parameter window whose size shrinks with the number of lattice sites [35–39]. If one breaks the homogeneity of the couplings, and considers a binary lattice, it was shown that there is a well-defined parameter window where $\mathcal{PT}$ symmetry is preserved [40].

A previous study of the effect of $\mathcal{PT}$ symmetry on Anderson localization, carried out on a (continuous) 2D square optical lattice, suggests that the system is always in the $\mathcal{PT}$-symmetric broken phase and, consequently, light localization is enhanced [41]. However, in Ref. [42] Bendix *et al.* found that for sufficiently long 1D chains, the system remains in the exact $\mathcal{PT}$-symmetric phase only inside an exponentially small parameter region. On the other hand, in Ref. [43], West *et al.* developed a theory for the critical gain or loss parameter separating unbroken from broken $\mathcal{PT}$ symmetry. They showed that chaos assists the unbroken $\mathcal{PT}$ phase.

In this work we are interested in examining the interplay between the simultaneous presence of disorder and $\mathcal{PT}$ symmetry, and how this affects the transport properties of extended excitations (plane waves) and the dynamical evolution of a completely localized excitation across a 1D binary lattice. Contrary to the conclusions suggested in [41], we will show that the presence of $\mathcal{PT}$ symmetry does not always assist localization. More specifically we will show that, for a disordered binary lattice, the presence of gain and loss tends to favor (inhibit) the transport of extended (localized) excitations.

II. MODEL

Let us consider a weakly coupled array of optical waveguides with binary couplings (cf. Fig. 1). In addition, each guide possesses a propagation constant whose real part can be random, and whose imaginary part is distributed across the array in a manner that satisfies the requirements of $\mathcal{PT}$ symmetry, that is, the gain [yellow (light gray) circles] or

_____
*ccmejia@googlemail.com
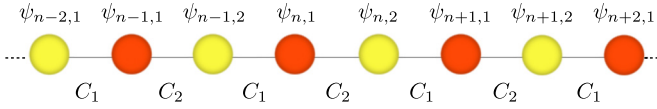
FIG. 1. (Color online) Sketch of the 1D linear binary lattice with alternating gain [yellow (light gray) filled circles] and loss [orange (dark gray) filled circles].

loss [orange (dark gray) circles] coefficient alternates in sign from site to site. Such a system can be modeled by a set of coupled, discrete linear Schrödinger equations. Considering only coupling between nearest-neighbor waveguides, the model is described by

$$i\frac{d\,\psi_{n,1}}{d\,z} + C_1\psi_{n-1,2} + C_2\psi_{n,2} + (\gamma_{n,1} + i\rho_{n,1})\psi_{n,1} = 0,$$
$$i\frac{d\,\psi_{n,2}}{d\,z} + C_1\psi_{n+1,1} + C_2\psi_{n,1} + (\gamma_{n,2} + i\rho_{n,2})\psi_{n,2} = 0,$$

(1)

with $\gamma_{n,1(2)} = 1 + \varepsilon_{n,1(2)}$. Here $\varepsilon_{n,1(2)}$ is a real random number and $\varepsilon_{n,1(2)} \in [-W/2, W/2]$ where W is the disorder width. A possible choice for the gain and loss coefficient $\rho_{n,1(2)}$ is to set $\rho_{n,1} = +\rho$ and $\rho_{n,2} = -\rho$.

The optical power content for such a system is defined as

$$P = \sum_n |\psi_{n,1}|^2 + |\psi_{n,2}|^2$$

(2)

and in the absence of gain and loss, P is a conserved quantity. Model (1) is a Hamiltonian system, where $id_z\psi_{n,1(2)} = \partial H/\partial\psi^*_{n,1(2)}$. The (non-Hermitian) Hamiltonian is given by

$$H = \sum_n [i\rho(|\psi_{n,1}|^2 - |\psi_{n,2}|^2) + C_2\psi^*_{n,1}\psi_{n,2}$$
$$+ C_1\psi^*_{n,1}\psi_{n-1,2} + C_2\psi^*_{n,2}\psi_{n,1} + C_1\psi^*_{n,2}\psi_{n+1,1}]. \quad (3)$$

In order to distinguish the spatial distribution (structure) of various solutions, a useful quantity called the participation rate of a solution $\psi_{n,1(2)}$ is defined as

$$R = \frac{P^2}{\sum_n |\psi_{n,1}|^4 + |\psi_{n,2}|^4},$$

(4)

which indicates how many sites are effectively excited in the lattice. Here n runs over a half of the total number of sites (N). For a completely extended state, $R = N$, while in the presence of complete localization, $R = 1$.

We begin by looking at the structure of the modes of the corresponding eigenvalue problem. As a first, and very rough preliminary view, we collapse the whole lattice to only two sites, i.e., a dimer, and examine the behavior of the instability gain of the modes as a function of the gain and loss parameter, and also as a function of the disorder width.

III. SIMPLIFIED DIMER MODEL

The corresponding equations for the dimer model in our system are

$$i\frac{d\,\psi_1}{d\,z} + (\varepsilon_1 + i\rho)\psi_1 + C\psi_2 = 0,$$
$$i\frac{d\,\psi_2}{d\,z} + (\varepsilon_2 - i\rho)\psi_2 + C\psi_1 = 0.$$

(5)

We look for stationary solutions $\psi_{1(2)}(z) \sim \psi_{1(2)} \exp(i\lambda z)$. This leads to the eigenvalue equation

$$(-\lambda + \varepsilon_1 + i\rho)\psi_1 + C\psi_2 = 0,$$
$$(-\lambda + \varepsilon_2 - i\rho)\psi_2 + C\psi_1 = 0.$$

(6)

After solving the eigenvalue problem, one obtains the propagation constant

$$\lambda = \frac{(\varepsilon_1 + \varepsilon_2)}{2} \pm \frac{1}{2}\sqrt{(\varepsilon_1 - \varepsilon_2)^2 - 4\rho^2 + 4C^2 + 4i(\varepsilon_1 - \varepsilon_2)\rho}.$$

(7)

In this oversimplified model, the disorder width is given by $|\varepsilon_1 - \varepsilon_2|$.

We note that λ is in general a complex number, but in the absence of "disorder," i.e., when $\varepsilon_1 = \varepsilon_2$, the system is $\mathcal{PT}$ symmetric and there is a parameter window where $\lambda \in \text{Re}$: $\rho < C$. We conclude that the presence of any amount of disorder gives rise to a complex propagation constant. Now, let us look at the behavior of the imaginary part of λ as a function of ρ, keeping the coupling constant, $C = 1$. From Eq. (7) we obtain the imaginary part of λ, or instability gain, as

$$g = \frac{1}{\sqrt{2}}(-a + \sqrt{a^2 + b^2})^{1/2},$$

(8)

where $a = (\varepsilon_1 - \varepsilon_2)^2 - 4\rho^2 + 4C^2$, $b = 4(\varepsilon_1 - \varepsilon_2)\rho$. Figure 2(a) shows the behavior of g as a function of ρ for several values of disorder width W.

Perhaps the most interesting feature of this graph is the fact that the instability gain increases as a function of disorder, for a fixed gain and loss parameter. At large enough ρ values, all the curves fall eventually on the $W = 0$ case: $g = \Theta(\rho - 1)\sqrt{\rho^2 - 1}$, where $\Theta(x)$ is the step function: $\Theta(x) = 0$ for $x < 0$, or $\Theta(x) = 1$ for $x > 0$.

Now, let us look at the behavior of the participation ratio R for our dimer system:

$$R = \frac{(1 + \alpha^2)^2}{1 + \alpha^4},$$

(9)

where $\alpha \equiv |\psi_2|^2/|\psi_1|^2$. Now, R ranges between 1 and 2; when R approaches either 1 on any of the sites, we are in the "localized regime," while a value of 2 indicates an "extended regime." From Eq. (6) one obtains

$$\alpha = \frac{\psi_2}{\psi_1} = \frac{\lambda - \varepsilon_1 - i\rho}{C},$$

(10)

where λ is given explicitly by Eq. (7). Figure 2(b) shows R vs ρ for several "disorder widths." For a given disorder an increase in gain and loss reduces R, while for a fixed gain and loss, an increase in disorder also decreases R. It would seem that the presence of gain and loss is effectively increasing the disorder, which reduces the spatial extent of the stationary mode.

Thus, from the results of the dimer model, we conclude that the interplay of $\mathcal{PT}$ symmetry and disorder tends to enhance the action of disorder, while at the same time it leads the system into the broken $\mathcal{PT}$-symmetry regime, for any amount of disorder.
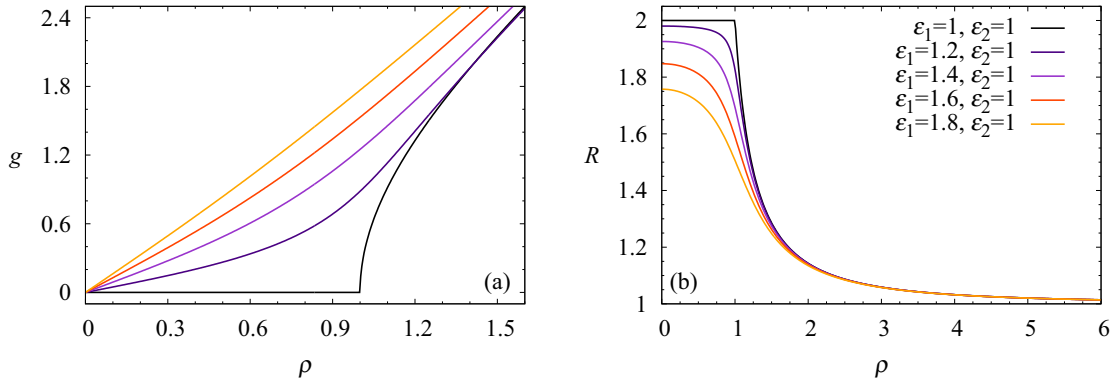
FIG. 2. (Color online) (a) Instability gain g and (b) participation ratio R in the dimer model, as a function of the gain and loss parameter ρ, both for several "disorder widths" labeled in the inset. $C = 1$.

IV. LONG WAVEGUIDE ARRAY

A. Gain and loss only

Now we consider a long waveguide array with N sites, with $N \gg 2$, described by model (1). We consider first the case of absence of disorder ($W = 0$), but in the presence of the gain and loss. We look for stationary modes of the form $\psi_{n,1(2)}(z) = \psi_{n,1(2)} e^{ikn + i\lambda z}$. This leads to the linear equations

$$(-\lambda + i\rho)\psi_{n,1} + (C_1 e^{-ik} + C_2)\psi_{n,2} = 0,$$
$$(C_2 + C_1 e^{ik})\psi_{n,1} + (-\lambda - i\rho)\psi_{n,2} = 0; \quad (11)$$

after imposing the condition that the determinant of the system be zero, in order for nontrivial solutions to exist, we arrive at the dispersion relation

$$\lambda_{\pm}(k,\rho) = \pm\sqrt{\Delta}, \quad (12)$$

where $\Delta \equiv C_1^2 + C_2^2 - \rho^2 + 2C_1 C_2 \cos k$. With this result we obtain the eigensolutions:

$$\begin{bmatrix} \psi_1^{\pm}, \\ \psi_2^{\pm} \end{bmatrix} = \begin{bmatrix} \delta_{\pm}, \\ 1 \end{bmatrix}, \quad \text{where,} \quad \delta_{\pm} = \frac{i\rho \pm \sqrt{\Delta}}{C_2 + C_1 e^{ik}}.$$

Stability domains or regions where the $\mathcal{PT}$ symmetry is preserved correspond to values of λ that are purely real. Inside the parameter window where this occurs, there is balance between gain and losses in the system.

Fixing $C_1 = 1$, and defining $C \equiv C_2/C_1$, we can rewrite the dispersion relation as

$$\lambda_{\pm}(k,\rho) = \pm\sqrt{-\rho^2 + 1 + C^2 + 2C \cos k}. \quad (13)$$

In order to guarantee that $\lambda \in \mathrm{Re}$, the relation $\rho^2 \leqslant 1 + C^2 + 2C \cos k$ must be fulfilled for all wave number k. Figure 3(a) shows the stability regions in parameters space, the $\rho - \mathrm{C}$ plane, for several wave vectors k. The different shaded areas represent stability domains for several k values. In particular there is a stability region valid for all k values, shown as the darkest region in Fig. 3(a). This is the most important case, since when one considers the dynamical evolution of a general optical excitation, each Fourier component will evolve according to one of the eigenvalues; if one or several of some of them are imaginary, the dynamics will be unstable. Thus, for stability it is necessary to stay inside the darkest region in Fig. 3(a). It is also worth pointing out that for the case of a homogeneous array, i.e., $C = 1$, there is no absolute stability window for any choice of parameters [40]. Figure 3(b) shows the instability gain defined as the maximum of the absolute value of all the imaginary parts of the eigenvalues. This instability gain will dominate the dynamics at long propagation distances. Under the curve we have indicated the character of the eigenvalues in different sectors of ρ values. For our normalization choice, the first region with real eigenvalues
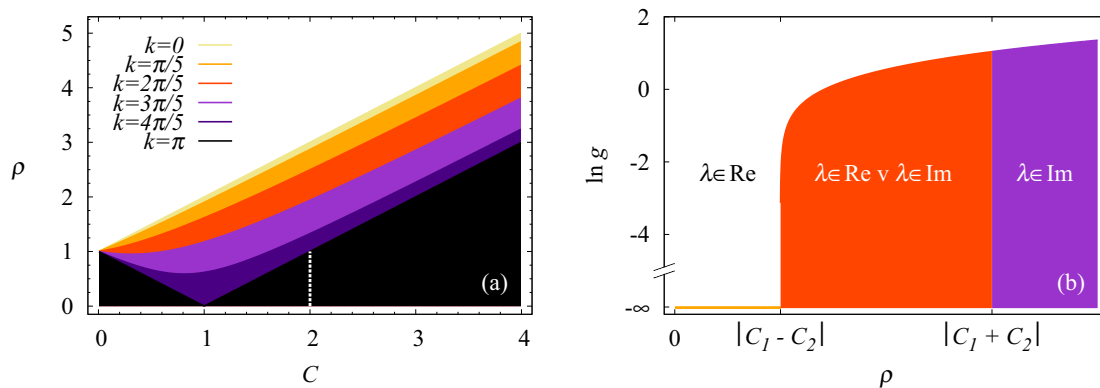
FIG. 3. (Color online) (a) Stability regions as function of gain and loss parameter ρ and coupling ratio C, for several wave vectors k. Darkness increases with k. Stable modes for all k ($\lambda \in \mathrm{Re}$) can only exist within the darkest region. (b) Instability gain g (log scale) as a function of gain and loss ρ, in the absence of disorder. The character of the eigenvalues changes with ρ.

only extends from $C = 0$ up to $C = 1$. Between $C = 1$ and $C = 3$, the eigenvalues are either real or imaginary, and finally for $C > 3$ the eigenvalues are all imaginary.

Let us now go deeper into the localization of the light for systems that exhibit a dispersion relation as from Eq. (12). We start by calculating the power content P of the corresponding eigenmodes,

$$P_\pm = \sum_n^N (1 + |\delta_\pm|^2) = \sum_{odd}^N 1 + \sum_{even}^N |\delta_\pm|^2 = \frac{1 + |\delta_\pm|^2}{2} N. \quad (14)$$

Therefore, the participation ratio R of an eigenmode is

$$R_\pm = \frac{(1 + |\delta_\pm|^2)^2}{1 + |\delta_\pm|^4} \frac{N}{2}. \quad (15)$$

We have two cases to consider. The first one corresponds to $\Delta \geqslant 0$, that is, inside the stable window. In that case, we have

$$R_\pm = \frac{\left[1 + \left(\frac{i\rho \pm \sqrt{\Delta}}{C_2 + C_1 e^{ik}}\right)\left(\frac{-i\rho \pm \sqrt{\Delta}}{C_2 + C_1 e^{-ik}}\right)\right]^2}{1 + \left[\left(\frac{i\rho \pm \sqrt{\Delta}}{C_2 + C_1 e^{ik}}\right)\left(\frac{-i\rho \pm \sqrt{\Delta}}{C_2 + C_1 e^{-ik}}\right)\right]^2} \frac{N}{2} = N. \quad (16)$$

In order to have an idea of the localization tendency of the whole system, we proceed to take an average over all eigenmodes, that is, an average over all wave vectors k:

$$\langle R_\pm \rangle^k = \frac{1}{2\pi} \int_0^{2\pi} R_\pm \, dk = N. \quad (17)$$

This means that the eigenmodes display complete delocalization in the $\mathcal{PT}$-symmetry phase. For the case $\Delta < 0$, we are in broken $\mathcal{PT}$-symmetry phase. The participation ratio is now

$$R_\pm = \frac{\left[1 + \left(\frac{i\rho \pm i\sqrt{-\Delta}}{C_2 + C_1 e^{ik}}\right)\left(\frac{-i\rho \mp i\sqrt{-\Delta}}{C_2 + C_1 e^{-ik}}\right)\right]^2}{1 + \left[\left(\frac{i\rho \pm i\sqrt{-\Delta}}{C_2 + C_1 e^{ik}}\right)\left(\frac{-i\rho \mp i\sqrt{-\Delta}}{C_2 + C_1 e^{-ik}}\right)\right]^4} \frac{N}{2},$$

$$= \frac{-N\rho^2}{C_1^2 + C_2^2 - 2\rho^2 + 2C_1 C_2 \cos k}, \quad (18)$$

and the mean participation ratio will be given by

$$\langle R_\pm \rangle^k = \frac{N}{2\pi} \int_0^{2\pi} dk \frac{-\rho^2}{C_1^2 + C_2^2 - 2\rho^2 + 2C_1 C_2 \cos k}. \quad (19)$$

Equation (19) establishes, in a closed form, the evolution of the participation rate for a binary lattice in terms of the strength of gain and loss parameter, as well as a function of the strength of its couplings. Figure 4(b) (upper curve) shows $\langle R \rangle^k$ as a function of ρ, in the absence of disorder. As ρ increases, $\langle R \rangle^k$ decreases, indicating a greater localization. This is reminiscent of Anderson localization with ρ playing the part of the disorder width, which is in qualitative agreement with recent experiments [33].

B. Gain and loss plus disorder

Let us now add disorder into the picture. The presence of disorder makes the system no longer $\mathcal{PT}$ symmetric, and some eigenvalues will be complex. Disorder also destroys the periodicity of the system and the computation of its eigenvalues and eigensolutions must proceed numerically. The instability gain, $g \equiv \text{Im}(\lambda)_{max}$, will dominate the dynamics at long propagation distances. Figure 4(a) shows this instability gain as a function of the gain and loss parameter, for several disorder widths labeled in the inset, and a coupling ratio of $C = 2$. In general, for a given disorder width, the gain increases monotonically with ρ, converging eventually to the curve $g(\rho) = \sqrt{\rho^2 - 1}$. On the other hand, for a fixed ρ, the gain also increases with disorder. This behavior of the gain suggests that the presence of disorder and gain and loss tends to destabilize the system. In Fig. 4(b) we show the participation ratio, this time averaged over all eigenstates and over a number of disorder realizations ($N_r = 100$). This double-averaged parameter serves as an estimator for the localization tendency of the system. As we can see, for a fixed gain and loss value, an increase in disorder decreases $\langle R \rangle_W^k$, indicating an increase in localization, as expected on general grounds. On the other hand, for a fixed disorder, $\langle R \rangle_W^k$ first increases with ρ, reaches a maximum, and finally decreases steadily with further increase in ρ. Note that the maximum occurs at $|C_1 - C_2| = 1$, and that there is an inflection point at $|C_1 + C_2| = 3$. We have seen these two special points before when examining the instability gain in the absence of disorder [Fig. 3(b)]. Now, the initial increase of $\langle R \rangle_W^k$ with ρ indicates that, as ρ is increased, the optical power content of the modes becomes more uniformly distributed in space. A very similar phenomenon has been observed in lattices with disorder and nonlinearity [44].
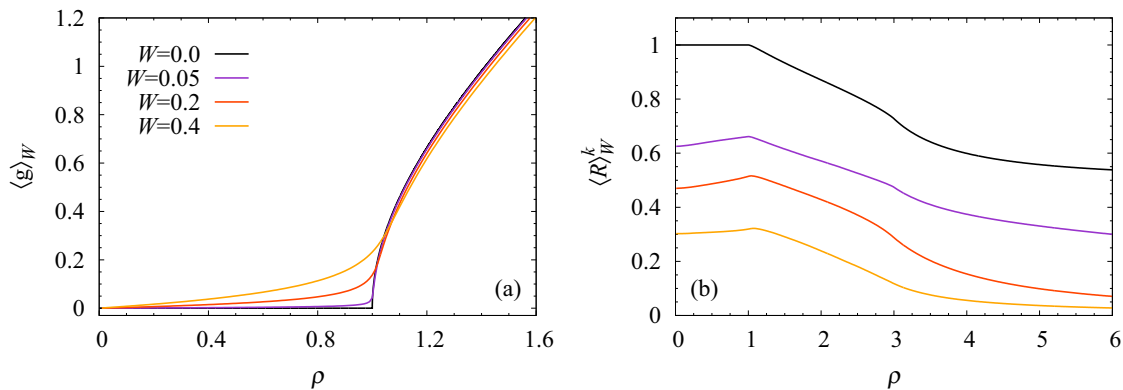
FIG. 4. (Color online) (a) Averaged instability gain $\langle g \rangle_W$ and (b) participation ratio R in a 1D binary array with disorder, gain, and loss, as a function of the gain and loss parameter ρ, both for several disorder widths labeled in the inset. $C = 2$.
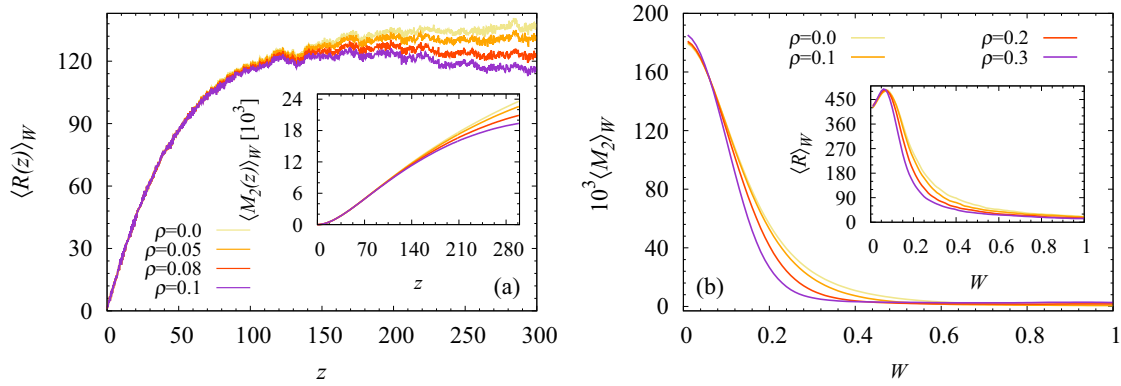
FIG. 5. (Color online) Dynamical wave-packet evolution in 1D binary array with disorder, gain, and loss. (a) $\langle R(z) \rangle_W$ and $\langle M_2(z) \rangle_W$ (inset) are displayed for several gain and loss values in the range $0 \leqslant \rho \leqslant 0.1$, and (b) $\langle M_2 \rangle_W$ and $\langle R \rangle_W$ (inset) as a function of W for several gain and loss values in the range $0 \leqslant \rho \leqslant 0.3$. $C = 2$.

V. TRANSPORT PROPERTIES

Let us now consider the problem of the transport of optical power in this binary waveguide array modeled by Eq. (1), originally $\mathcal{PT}$ symmetric, and then slightly perturbed by introducing disorder into their propagation constants, that is by imposing a random distribution of indices of refraction. We will focus on two cases: the propagation of initially localized (δ-function-like) and of extended (plane wave) excitations.

A. δ-like beam excitation

We start by analyzing the dynamical evolution of a narrow input beam focused on the central guide of the array. For that we integrate numerically the model (1), for a binary waveguide array in the presence of alternating gain and losses and linear disorder. We will focus on the mean size of the wave packet upon the beam propagation, measured by the mean-square displacement,

$$M_2 = \frac{\sum_{i=1}^{N}(n - n_c)^2 |\psi_i|^2}{\sum_{i=1}^{N} |\psi_i|^2}. \tag{20}$$

In our simulations, we take $N = 1200$, and $n_c = N/2$ is the initially excited waveguide. It is worth mentioning that model (1) (for $\rho \neq 0$) is a non-Hermitian system, then, there is no conserved quantities (integrals of motion) during propagation. For instance, the optical power $P = \sum_n |\psi_n|^2$ is not a dynamical constant and we expect that, in the absence of disorder, its value will oscillate. However, in the presence of disorder the $\mathcal{PT}$ symmetry could be broken leading to the growth of the optical power.

Since we are dealing with disordered arrays, we must collect information from a number N_r of different disorder realizations, and then take the average over them. Quantities (2) and (4) are also useful in that they tell us how the light is distributing along the array upon propagation. In the following numerical analysis, we have set a coupling ratio of $C = 2$ and, for each case, we perform 100 disorder realizations ($N_r = 100$). In the absence of disorder, the $\mathcal{PT}$ symmetry will hold for $\rho \leqslant 1$ [see white dotted line in Fig. 3(a)]. However, the interplay between gain and losses with disorder breaks

the $\mathcal{PT}$ symmetry, which could lead to the emergence of eigenfunctions with complex eigenvalues.

Figure 5(a) displays four cases of $\langle R(z) \rangle_W$ evolution for disordered binary arrays of length $z = 300$. Each of them corresponds to a different value of ρ parameter, but keeping the same width of disorder $W = 0.3$. The brightest line stands for $\rho = 0$, i.e., in the absence of gain and losses. The other lines correspond to $\rho = 0.05$, 0.08, and 0.1, respectively. From here, we clearly see how $\langle R(z) \rangle_W$ tends to saturate due to wave-packet localization, in agreement with the thesis of Anderson. Nevertheless, the number of effectively excited sites diminishes with the increment of ρ values, i.e., the presence of alternate gain and losses contributes to localize the wave packet further. Similarly, from the inset in Fig. 5(a) we observe that $\langle M_2(z) \rangle_W$ also evolves towards a saturation as expected from Anderson localization. It is worth pointing out here that the behavior described above is invariant against a spatial permutation that exchanges the sites with gain and loss. In other words, it does not matter whether the initial δ excitation is placed on a "gain" site or on a "loss" site.

Figure 5(b) shows the effect of disorder on the width of the wave packet $\langle M_2(z) \rangle_W$ at the output of an array of length $z = 100$, for several values of the gain and loss parameter. In all cases, as the width of the disorder increases, $\langle M_2(z) \rangle_W$ decreases steadily, as a power law. This decrease is faster for larger values of ρ. The behavior of the average participation ratio as a function of disorder, displayed as an inset in Fig. 5(b), is the same behavior, except at small disorder widths where R increases with W, for all ρ. We have noticed a similar behavior for R when we discussed Fig. 3. In other words, for small disorder widths there is a tendency to redistribute the optical power content in a more uniform manner among the guides [44].

B. Extended beam excitation

Finally, we analyze the averaged transmission $\langle T \rangle_W^k$ of a plane wave across a disordered segment of length L containing gain and losses, as well as disorder. We assume the segment embedded in a large homogeneous 1D lattice (black filled circles). A sketch of the system is shown in Fig. 6, where orange and yellow (light gray and dark gray) filled circles represent those sites with losses and gain, respectively.
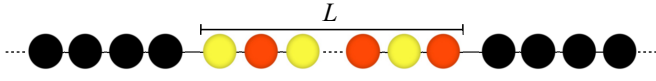
FIG. 6. (Color online) Sketch of a disordered segment, of length L, with alternating gain [yellow (light gray) filled circles] and losses [orange (dark gray) filled circles], embedded in a 1D linear homogeneous lattice (black filled circles).

We are interested in knowing how the transmissivity, as a function of L, is affected by the interplay of disorder and the presence of gain and loss. In the absence of gain and loss, it is well known that the transmission would decay exponentially with the size of the disordered segment [45]. When disorder and nonlinearity are present, the transmission decays as a power law [46].

Outside the "impurity" segment, the system is modeled by the discrete Schrödinger equation,

$$\frac{d\psi_n}{dz} + V(\psi_{n-1} + \psi_{n+1}) = 0, \qquad (21)$$

which has stationary solutions of the form $\psi_n = \phi_n e^{i\lambda z}$, leading to the dispersion relation $\lambda = 2V \cos k$. On the other hand, inside the segment, the field is governed by model (1), which can be rewritten in the following way:

$$i\frac{d\psi_n}{dz} + C_{n,n-1}\psi_{n-1} + C_{n,n+1}\psi_{n+1} + \gamma_n \psi_n = 0, \qquad (22)$$

where now $\gamma_n = 1 + \varepsilon_n \pm i\rho_n$, with $\rho_n = \rho\ (-\rho)$ for n even (odd). Its stationary version is given by

$$\lambda\phi_n + C_{n,n-1}\psi_{n-1} + C_{n,n+1}\psi_{n+1} + \gamma_n \psi_n = 0. \qquad (23)$$

Let us now consider the transmission of an extended excitation, i.e., a plane wave across the segment:

$$\psi_n = \begin{cases} R_0 e^{ikn} + R_1 e^{-ikn}, & n \leqslant 0, \\ R_2 e^{ikn}, & n \geqslant L. \end{cases} \qquad (24)$$

From Eq. (23), we obtain the recurrence relation

$$\psi_{n-1} = \frac{(\lambda - \gamma_n)\psi_n - C_{n,n+1}\psi_{n+1}}{C_{n,n-1}}, \qquad (25)$$

which we will use to compute the transmission: for a given wave vector k, one starts at the end of the segment $n = L$ and

assumes a given value for R_2. For example $R_2 = 1$. Therefore, from Eq. (24), at $N = L$ and $n = L + 1$, $\psi_L = \exp(ikL)$ and $\psi_{L+1} = \exp[ik(L+1)]$, respectively. Then we iterate backwards using the above recurrence relation, Eq. (25), until we reach the beginning of the segment where R_0 is computed. The transmissivity is then given by $T = |R_2|^2/|R_0|^2$.

Figure 7 shows the average transmission (log scale) across a disordered segment of length L, with gain and losses. We have averaged over 100 disorder realizations, and also over all wave vectors k. In general, we see that $\langle T \rangle_W^k$ decreases with L, and this tendency is stronger when the width of disorder increases. This is shown in Fig. 7(b), where light gray (gray and dark gray) lines correspond with $W = 0.1$ ($W = 0.2$ and 0.3).

Figure 7(a) shows something interesting: as the gain and loss coefficient is increased (for fixed disorder and fixed L), the transmission increases with ρ. This is in marked contrast to the case of the δ-like beam excitation where the opposite tendency occurred. We also observe the presence of fluctuations in the transmission, some of them becoming quite strong ($T \gg 1$), for a specific impurity length. We point out here that this kind of fluctuation also appears in the absence of disorder. For those values of ρ within the stability zone [Fig. 3(a)], but not so close to the boundary, the total transmission slightly oscillates around values lower than unity. However, values of ρ close to the boundary and beyond, lead to strong fluctuations around specific system lengths. Therefore, the system leaves the $\mathcal{PT}$-symmetric regime as soon as disorder is imprinted in the system. To these fluctuations correspond regimes of very strong amplification.

VI. DISCUSSION

We have examined the transport of excitations across a 1D binary lattice, in the presence of disorder, plus the presence of gain and loss. In the absence of disorder, the system is $\mathcal{PT}$ symmetric. As a first approach to the problem we studied a dimer reduction, observing that the interplay of $\mathcal{PT}$ symmetry and disorder tends to enhance the action of disorder, while at the same time it leads the system into the broken $\mathcal{PT}$-symmetry regime, for any amount of disorder. Next, we examine the case of a long binary lattice, finding that as soon as disorder is introduced, the system goes into the broken
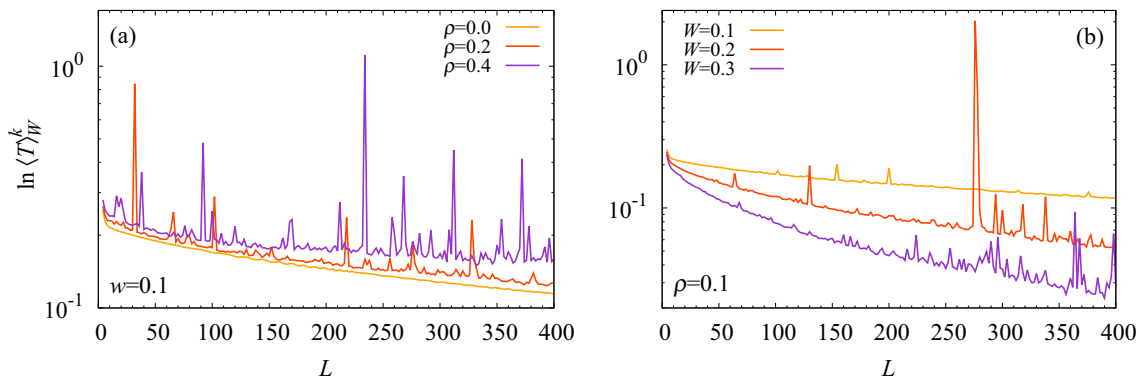
FIG. 7. (Color online) Averaged transmission $\langle T \rangle_W^k$ of a plane wave across a disordered segment containing gain and loss, as a function of the length of the segment L. (a) $\rho = 0.0$ ($\rho = 0.2$ and $\rho = 0.4$) lower (middle and upper) curve for fixed $W = 0.1$, and (b) $W = 0.1$ ($W = 0.2$ and $W = 0.3$) upper (middle and lower) line for fixed $\rho = 0.1$.

$\mathcal{PT}$-symmetry phase, and that the presence of gain and loss tends to reinforce the action of disorder.

Next we consider the propagation of localized and extended excitations inside the binary system. For the case of the δ-like initial beam, we observe that its propagation is somewhat inhibited by an increase in gain and loss. Surprisingly, the opposite happens when examining the transmission of plane waves across a binary lattice segment with disorder and gain and loss: in that case, the presence of gain and loss tends to increase the transmission. This transmission experiments robust fluctuations over imposed over its well-defined decaying behavior as the segment length increases. These fluctuations appear independent of the width of disorder or the strength of gain and loss parameter. Moreover, we have observed fluctuations for the case of a fixed ρ and L and varying disorder W. We believe that the origin of these fluctuations with L or W have their origin in the complex eigenvalue spectra of the system. For a fixed ρ and L, the set of eigenvalues will change from random realization to realization, introducing new instability gains which might cause the transmission to change abruptly. On the other hand, for a system with fixed disorder and gain and loss, a change in L, generates a different set of complex eigenvalues where, again, the instability gain might change, even for as small a change as one site. The fluctuations can become so strong as to generate transmissions greater than unity (see Fig. 7).

We conclude that, for a binary chain, the interplay of disorder and gain and loss tends to reduce the spatial extent of the eigenmodes and that it favors (inhibits) the dynamical propagation of extended (localized) excitations, giving also rise to strong fluctuations in the transmission of plane waves across the system.

[1] P. W. Anderson, Phys. Rev. **109**, 1492 (1958).

[2] M. H. Cohen, H. Fritzsche, and S. R. Ovshinsky, Phys. Rev. Lett. **22**, 1065 (1969).

[3] N. F. Mott, Philos. Mag. **19**, 835 (1969).

[4] I. Lifshits, S. Gredeskul, and L. Pastur, *Introduction to the Theory of Disordered Systems* (Wiley, New York, 1988).

[5] P. Sheng, *Scattering and Localization of Classical Waves in Random Media*, World Scientific Series on Directions in Condensed Matter Physics (World Scientific, Singapore, 1990).

[6] S. Ping, *Introduction to Wave Scattering, Localization and Mesoscopic Phenomena* (Academic Press, San Diego, 2006).

[7] R. Weaver, Wave Motion **12**, 129 (1990).

[8] D. Photiadis, J. Acoust. Soc. Am. **88**, S21 (1990).

[9] J. Billy, V. Josse, Z. Zuo, A. Bernard, B. Hambrecht, P. Lugan, D. Clément, L. Sanchez-Palencia, P. Bouyer, and A. Aspect, Nature (London) **453**, 891 (2008).

[10] S. John, Phys. Rev. Lett. **53**, 2169 (1984).

[11] V. Freilikher and S. Gredeskul, *Progress in Optics* (Elsevier, Amsterdam, North-Holland, 1992), Vol. 30, pp. 137–203.

[12] D. S. Wiersma, P. Bartolini, A. Lagendijk, and R. Righini, Nature (London) **390**, 671 (1997).

[13] T. Schwartz, G. Bartal, S. Fishman, and M. Segev, Nature (London) **446**, 52 (2007).

[14] Y. Lahini, A. Avidan, F. Pozzi, M. Sorel, R. Morandotti, D. N. Christodoulides, and Y. Silberberg, Phys. Rev. Lett. **100**, 013906 (2008).

[15] U. Naether, S. Sttzer, R. A. Vicencio, M. I. Molina, A. Tnnermann, S. Nolte, T. Kottos, D. N. Christodoulides, and A. Szameit, New J. Phys. **15**, 013045 (2013).

[16] M. Segev, Y. Silberberg, and D. N. Christodoulides, Nat. Photon. **7**, 197 (2013).

[17] C. M. Bender and S. Boettcher, Phys. Rev. Lett. **80**, 5243 (1998).

[18] C. M. Bender, D. C. Brody, and H. F. Jones, Phys. Rev. Lett. **89**, 270401 (2002).

[19] R. El-Ganainy, K. G. Makris, D. N. Christodoulides, and Z. H. Musslimani, Opt. Lett. **32**, 2632 (2007).

[20] Z. H. Musslimani, K. G. Makris, R. El-Ganainy, and D. N. Christodoulides, Phys. Rev. Lett. **100**, 030402 (2008).

[21] K. G. Makris, R. El-Ganainy, D. N. Christodoulides, and Z. H. Musslimani, Phys. Rev. Lett. **100**, 103904 (2008).

[22] A. Guo, G. J. Salamo, D. Duchesne, R. Morandotti, M. Volatier-Ravat, V. Aimez, G. A. Siviloglou, and D. N. Christodoulides, Phys. Rev. Lett. **103**, 093902 (2009).

[23] C. E. Rüter, K. G. Makris, R. El-Ganainy, D. N. Christodoulides, M. Segev, and D. Kip, Nat. Phys. **6**, 192 (2010).

[24] A. E. Miroshnichenko, B. A. Malomed, and Y. S. Kivshar, Phys. Rev. A **84**, 012123 (2011).

[25] A. Regensburger, C. Bersch, M.-A. Miri, G. Onishchukov, D. N. Christodoulides, and U. Peschel, Nature (London) **488**, 167 (2012).

[26] C. M. Bender, M. Gianfreda, S. K. Özdemir, B. Peng, and L. Yang, Phys. Rev. A **88**, 062111 (2013).

[27] J. Schindler, A. Li, M. C. Zheng, F. M. Ellis, and T. Kottos, Phys. Rev. A **84**, 040101 (2011).

[28] N. Hatano and D. R. Nelson, Phys. Rev. Lett. **77**, 570 (1996).

[29] Y. N. Joglekar, D. Scott, M. Babbey, and A. Saxena, Phys. Rev. A **82**, 030103 (2010).

[30] N. Lazarides and G. P. Tsironis, Phys. Rev. Lett. **110**, 053901 (2013).

[31] A. Szameit, M. C. Rechtsman, O. Bahat-Treidel, and M. Segev, Phys. Rev. A **84**, 021806 (2011).

[32] B. Peng, S. K. Ozdemir, F. Lei, F. Monifi, M. Gianfreda, G. L. Long, S. Fan, F. Nori, C. M. Bender, and L. Yang, Nat. Phys. **10**, 394 (2014).

[33] T. Eichelkraut, R. Heilmann, S. Weimann, S. Stützer, F. Dreisow, D. N. Christodoulides, S. Nolte, and A. Szameit, Nat. Commun. **4**, 2533 (2013).

[34] G. Tsironis and N. Lazarides, Appl. Phys. A **115**, 449 (2014).

[35] D. D. Scott and Y. N. Joglekar, Phys. Rev. A **83**, 050102 (2011).

[36] I. V. Barashenkov, L. Baker, and N. V. Alexeeva, Phys. Rev. A **87**, 033819 (2013).

[37] M. I. Molina, Phys. Rev. E **89**, 033201 (2014).

[38] P. Kevrekidis, D. Pelinovsky, and D. Tyugin, SIAM J. Appl. Dyn. Syst. **12**, 1210 (2013).

[39] D. E. Pelinovsky, D. A. Zezyulin, and V. V. Konotop, J. Phys. A: Math. Theor. **47**, 085204 (2014).

[40] S. V. Dmitriev, A. A. Sukhorukov, and Y. S. Kivshar, Opt. Lett. **35**, 2976 (2010).

[41] D. M. Jović, C. Denz, and M. R. Belić, Opt. Lett. **37**, 4455 (2012).

[42] O. Bendix, R. Fleischmann, T. Kottos, and B. Shapiro, Phys. Rev. Lett. **103**, 030402 (2009).

[43] C. T. West, T. Kottos, and T. Prosen, Phys. Rev. Lett. **104**, 054102 (2010).

[44] U. Naether, S. Rojas-Rojas, A. J. Martínez, S. Stützer, A. Tünnermann, S. Nolte, M. I. Molina, R. A. Vicencio, and A. Szameit, Opt. Express **21**, 927 (2013).

[45] E. Economou, *Green's Functions in Quantum Physics*, Springer Series in Solid-State Sciences (Springer-Verlag, Berlin, Heidelberg, 2006).

[46] M. I. Molina, Phys. Rev. B **58**, 12547 (1998).